Synthesis and Evaluation of Indenopyrazoles as Cyclin-Dependent Kinase Inhibitors. 2. Probing the Indeno Ring Substituent Pattern

David A. Nugiel,* Anup Vidwans, Anna-Marie Etzkorn, Karen A. Rossi, Pamela A. Benfield, Catherine R. Burton, Sarah Cox, Deborah Doleniak, and Steven P. Seitz

Bristol-Myers Squibb Company, Box 80336, Wilmington, Delaware 19880-0336

We disclose a novel series of indenopyrazole-based cyclin-dependent kinase (CDK) inhibitors. Kinetic experiments confirmed our initial molecular modeling studies that the compounds are competitive with respect to adenosine 5′-triphosphate (ATP) and bind in the kinase ATP pocket. A unique combination of active pharmacophores led us to a series of semicarbazide-based inhibitors that are highly potent against CDK2 and CDK4 while maintaining selectivity against other relevant serine/threonine kinases. These compounds were active against a transformed human colon cancer cell line (HCT116) while maintaining an acceptable margin of activity against a normal fibroblast cell line. The compounds were found to be highly protein bound in our cell-based assay with the exception of **11k**, which maintained a reasonable level of activity in the presence of human plasma proteins.
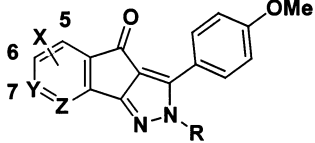
Introduction

One of the most important and fundamental processes in biology is the replication of genetic information, which occurs during cell division. The cell cycle machinery mediates replication of DNA and its accurate distribution to daughter cells. Deregulation of this machinery can lead to uncontrolled or aberrant proliferation commonly observed in the generation of tumors.[1]

The cyclin-dependent kinases (CDKs) represent core components of the cell cycle regulatory machinery. Each CDK associates with a specific cyclin regulatory partner to generate the active catalytic moiety. The coordinate activity of different CDKs guides individual cells through the replication process and ensures the vitality of each subsequent generation.[2]

The products of several prominent oncogenes and tumor suppressor genes play important roles in cell cycle control. An increasing body of evidence indicates that uncontrolled CDK activity is a common feature of tumor development.[3] This realization has prompted the search for small molecule inhibitors of the CDK family of enzymes as a possible approach to cancer chemotherapy.[4] Several disclosures have discussed small molecules with CDK inhibitory activity.[5] Two compounds (Flavopiridol and UCN-01) have entered advanced clinical trials as cancer therapeutics based on this CDK inhibition mechanism.[6]

We recently disclosed a new structural class of potent and selective CDK inhibitors, which were active against transformed cell lines and showed in vivo activity in a human xenograft model.[7] High throughput screening (HTS) of our compound collection against CDK4/D1 uncovered several interesting leads including **1** (Table 1). Subsequent screening of this hit against other members of the CDK family as well as other relevant serine/threonine kinases revealed the compound to have selectivity for the CDK family. We began a medicinal

Table 1. Enzymatic Activity for Indeno-Core Analogues

| compd	X	Y	Z	R	CDK4/D1 IC$_{50}$ (μM)^a	CDK2/E IC$_{50}$ (μM)^a
1	H	C	C	H	45	26
3a	H	C	C	Me	>340	>340
3b	6-OH	C	C	H	21.5	NM^b
3c	5-acetamide	C	C	H	0.46	0.51
3d	5-OH	C	C	H	20	5.2
3e	6-acetamide	C	C	H	>150	>300
3f	6-NH$_2$	C	C	H	108	210
4	5-NH$_2$	C	C	H	23	8.4
3g	H	C	C	Ph	>200	>280
3h	H	N	C	H	34.5	4.7
3i	C$_4$H$_4$	C	C	H	80	NM^b
3j	H	C	N	H	>361	NM^b
3k	6,7-Cl	C	C	H	55.5	NM^b

^{a} Values correspond to $n = 2$. ^{b} NM = not measured. For assay conditions, see Experimental Section.

chemistry effort around **1** in an attempt to improve potency against the CDK family while maintaining a favorable selectivity profile. This paper provides details of that study with regards to optimizing the indenopyrazole core. Specifically, the emphasis will be on the structure–activity relationships (SAR) relevant to the indeno portion of the core structure as well as substituents at the 5-postion of the indeno ring, which proved to be key for enhanced activity against the CDK family. The following paper will detail the discovery of substituents at the 3-position of the indenopyrazole core and novel chemical methods for synthesizing those analogues.[8]
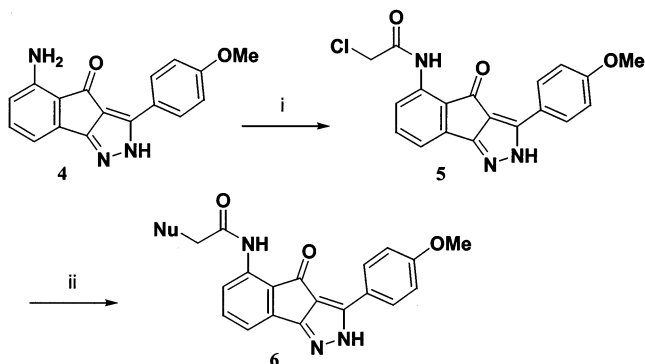
Chemistry

Kilgore et al. disclosed the synthesis of **2** in 1941.[9] Attempts at reproducing this chemistry gave low yields

* To whom correspondence should be addressed. Tel: 302-467-5847. Fax: 302-467-6772. Email: david.nugiel@bms.com.

Scheme 1[a]
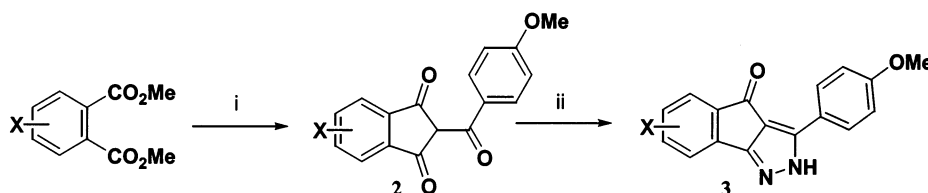
[a] Reagents and conditions: (i) NaH, 4-methoxyacetophenone, DMF, 90 °C, 50%. (ii) Hydrazine, catalytic *p*-TsOH, EtOH, reflux, 50%.

Scheme 2[a]

[a] Reagents and conditions: (i) ClCH₂C(O)Cl, acetone, NaHCO₃, 50 °C, 75%. (ii) Nucleophile, NaHCO₃, acetone, 75−90%.

Scheme 3[a]

[a] Reagents and conditions: (i) Concentrated HCl, MeOH, reflux, 86%; (ii) PhOC(O)Cl, Na₂CO₃, acetone, 50 °C, 78%. (iii) Nucleophile, DMSO, 80 °C, 85−95%. (iv) Hydrazine, catalytic *p*-TsOH, EtOH, reflux, 45%.

of the desired tricarbonyl intermediate (**2**, X = H), and we subsequently modified the synthetic method as shown in Scheme 1. Treating the appropriate phthalate ester with sodium hydride and 4-methoxyacetophenone at 90 °C in dimethylformamide (DMF) gave a good yield of the desired tricarbonyl intermediate **2**. This intermediate was treated with hydrazine and a catalytic amount of *p*-toluenesulfonic acid (pTsOH) in refluxing ethanol for 2 h to give the final target indenopyrazole **3**. The yield for this reaction varied between 40 and 60% depending on the starting phthalate ester substitution pattern.

The synthesis of **3c** (Table 1) was disclosed previously[7] and led to the need for additional analogues substituted at the 5-postion of the indenopyrazole core. The synthesis of those analogues is described in Scheme 2 starting from the advanced intermediate **4**. Treating aniline **4** with chloroacetyl chloride and NaHCO₃ in acetone at 50 °C gave the α-chloroacetamide **5** in 75% yield. This advanced intermediate was very versatile, and we were able to generate a small library of glycinamide analogues using a variety of nitrogen-based nucleophiles. Treating intermediate **5** with the desired nucleophile in acetone and NaHCO₃ gave the desired glycinamides **6** in good overall yield.

The synthesis of urea and semicarbazide-containing analogues is described in Scheme 3. The preparation of advanced intermediate **7** was described previously.[7] Deacylation of the amide using concentrated HCl in refluxing methanol gave the desired aniline in quantitative yield. This aniline was converted to the corresponding phenyl carbamate in good yield using phenylchloroformate in acetone at room temperature. This key intermediate was used to make a variety of ureas and semicarbazides depending on the choice of nucleophile. Heating intermediate **9** in dimethyl sulfoxide (DMSO) with the appropriate nucleophile gave the desired product in good to excellent yield. Using DMSO as the
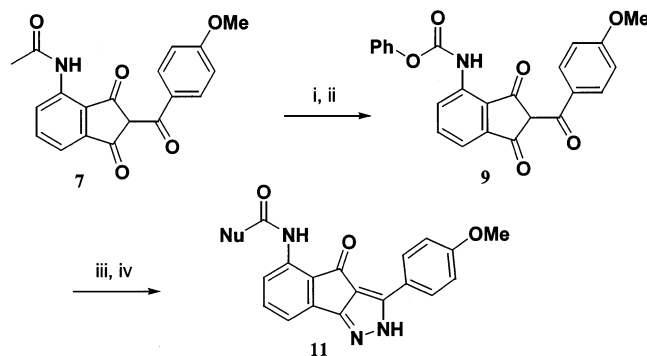
solvent for this reaction was critical. Dichloromethane, tetrahydrofuran (THF), and dioxane were all tried and gave no conversion to the desired product. Final closure to the pyrazole was accomplished using the same reaction conditions as described above to give the indenopyrazoles in good yield.

Results and Discussion

Initial SAR. Our initial efforts focused on modifying the indenopyrazole core of **1** to try and maintain our selectivity profile and improve binding affinity for CDK2 and CDK4 (Table 1). Early on, we realized that the pyrazole NH provided a key interaction with the enzyme. To maintain any level of activity, we could not substitute at this position at all (**3a,g**). Enlarging the aromatic portion of the indenopyrazole core (**3i**) did not improve activity, but activity did not disappear entirely. This analogue gave some indication as to the size of the binding pocket that these compounds occupied. Replacing the naphthyl moiety with two chlorines (**3k**) did not improve activity and generated an inactive analogue.

Attempts at picking up hydrogen bond interactions by introducing nitrogens into the indeno aromatic core met with mixed results. The 8-aza analogue **3j** was essentially inactive, but the 7-aza analogue **3h** gave similar activity against CDK4 and about a 5-fold improvement against CDK2 as compared with **1**.

Our next attempt was to introduce hydrogen bond donating substituents to the core. Both the 5-hydroxy and the 6-hydroxy analogues (**3b,d**) gave modest increases in activity suggesting that this would be a productive path to follow. We were concerned that introducing additional phenolic hydroxy groups into the molecule could effect the selectivity profile of this series by initiating tyrosine kinase inhibitory activity. Both hydroxy analogues **3b,d** showed increased affinity toward tyrosine kinases in our selectivity panel.[10] By
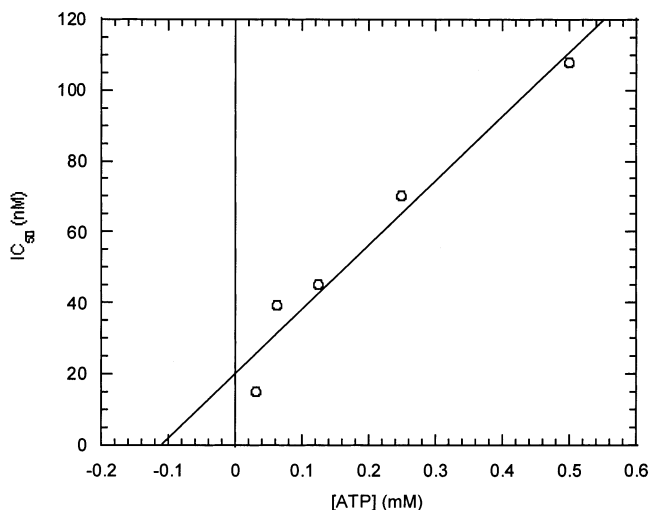
Figure 1. IC_{50} values for **6c** depend on ATP concentration. IC_{50} values were calculated by curve fitting; see Experimental Section.

Figure 2. Molecular model of **3c** docked in the ATP binding pocket of a CDK4/D1 homology model. The inhibitor is color-coded by atom type where carbon is yellow, oxygen is red, and nitrogen is blue. The enzyme is color-coded by atom type in a similar fashion except that carbon is green. Key enzyme residues and hydrogen bonds are labeled.

substituting amino groups for the hydroxy groups, we envisioned minimizing this potential problem while maintaining good hydrogen bond donating subtituents.

To this end, we targeted the preparation of the two anilino analogues **3f** and **4**. Neither of these compounds gave the potency improvement we had hoped for, but a surprise was waiting for us in one of the precursors to these targets. Compound **3c** was the first analogue to break the micromolar potency barrier and give us a compound with a CDK4 IC_{50} of 460 nM and a CDK2 IC_{50} of 510 nM. With our acetamide pharmacophore in hand, we were able to envision many new analogues with which we hoped to improve potency against our kinase targets.

Molecular Modeling. Several reports have been published describing the X-ray crystal structure of CDK2 complexed with adenosine 5′-triphosphate (ATP) and other small molecule inhibitors of this enzyme.[11] Other studies have shown insignificant structural changes in the ATP binding pocket of this kinase as a result of binding its cyclin regulatory units.[12] These reports suggest that information obtained from isolated CDK/inhibitor complexes can shed light on inhibitor design that would translate to active molecules against the kinase/cyclin complex.[13]

To date, no X-ray crystallographic information is available regarding the structure of CDK4. We were interested in gaining further insight as to how our series of CDK inhibitors bound to the ATP binding pocket of CDK4. Because many small molecule inhibitors of CDKs are competitive with ATP for binding, we reasoned that our series was also competitive with ATP. Kinetic studies with **6c** (Figure 1) support the assumption that our molecules are competitive with ATP and most likely bind in the enzyme's ATP binding pocket.

Using the crystal structure of CDK2/cyclinA as a starting point, we constructed a homology model of the CDK4/cyclin D complex and docked compound **3c** in the ATP binding pocket of the enzyme (Figure 2). Several key features are notable and support the SAR observed in this series. The molecule is buried deep in the ATP binding pocket as the two pyrazole nitrogens create key backbone hydrogen bonds with Val 96. The pyrazole NH
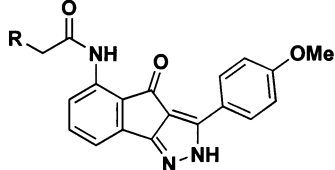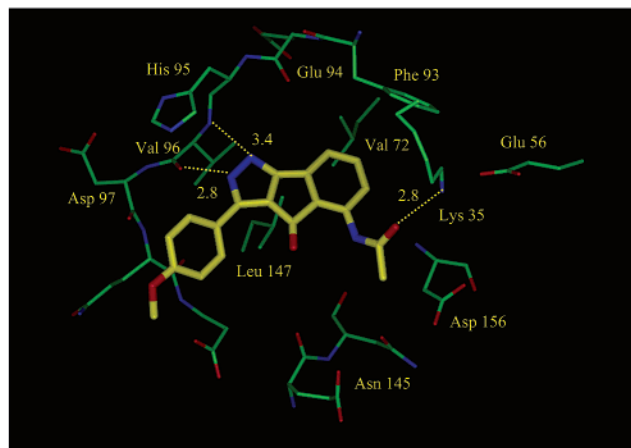
creates a 2.8 Å bond with the backbone carbonyl of Val 96, and the adjacent pyrazole nitrogen accepts a complementary bond from the same amino acid backbone NH at 3.4 Å. These key interactions are very similar to those seen in the X-ray crystal structure of olomoucine in the ATP binding pocket of CDK2.[14] Another key hydrogen bond is formed between the 5-substituted acetamide carbonyl and the side chain NH_2 group of Lys 35. This interaction could explain the significant jump in potency seen for compound **3c** relative to the other analogues in Table 1 that lack a substituent capable of creating this hydrogen bond.

The model suggests that the indeno ring carbonyl lacks any significant interactions with the enzyme and simply helps align the acetamide group through an intramolecular hydrogen bond with the adjacent amide NH. The indeno aromatic ring is buried deep in the pocket and has van der Waals interactions with several residues that line the pocket (Val 72, Phe 93, and Leu 147). The *p*-methoxyphenyl C-3 substituent projects outward toward the solvent-exposed area of the binding pocket and does not make any additional hydrophobic interactions with residues in this portion of the pocket.

Optimizing Enzymatic and In Vitro Potency. Preliminary studies had shown that small, linear substituents on the acetamide carbon were preferred. Branching at this α-carbon or direct substitution with an aromatic ring drastically reduced the compound's activity against the desired targets. Potent compounds are prepared by maintaining a methylene spacer between the acetamide carbonyl and the desired substituent to be introduced. The reactivity of aniline **4** precluded the use of standard amide bond coupling reactions to obtain the desired acetamide derivatives. Activating the acidic coupling partner as the acid chloride was the only synthetic method that consistently gave good results. The chloroacetamide intermediate **5** proved to be a very useful advanced intermediate to prepare a variety of glycinamide analogues (Table 2).

A variety of phenacetyl derivatives, exemplified by **6a**,[7] were prepared, and many had similar affinity for CDK2 and CDK4 as compared to **6a**. The SAR arising from these analogues indicated that the binding pocket

Table 2. Enzymatic Activity for Glycinamide Analogues

compd	R	CDK4/D1 IC$_{50}$ (μM)^a	CDK2/E IC$_{50}$ (μM)^b
6a	4-NH$_2$C$_6$H$_4$	0.48	0.038
6b	NH$_2$	>1.4	>0.72
6c	(Me)$_2$N	0.90	0.044
6d	piperazine	0.113	0.033
6e	1-piperidine	>1.0	0.185
6f	ethylNH	0.917	0.13
6g	thiomorpholine	>0.5	0.054
6h	morpholine	0.195	0.021
6i	*N*-methylpiperazine	0.125	0.012
6j	4-aminomethylpiperidine	0.02	0.012
6k	4-amidopiperidine	0.076	0.008
6m	4-hydroxymethylpiperidine	0.082	0.011
6n	4-amidopiperazine	0.064	0.008
6p	4-amidinopiperazine	0.026	0.007

^{a} Values correspond to $n = 2$. ^{b} Values correspond to $n = 2$. For assay conditions see Experimental Section.

Table 3. Enzymatic Activity for Urea/Semicarbazide Analogues

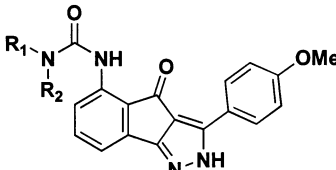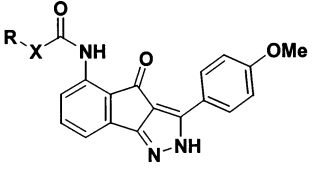| compd	R$_1$	R$_2$	CDK4/D1 IC$_{50}$ (μM)^a	CDK2/E IC$_{50}$ (μM)^b
11a	H	H	0.066	0.007
11b	ethyl	ethyl	>1.3	>1.3
11c	benzyl	H	0.307	0.095
11d	benzyl	Me	>2.3	>2.3
11e	4-picolyl	H	1.15	0.029
11f	4-methoxybenzyl	H	>1.1	0.180
11g	phenyl	H	0.877	0.032
11h	*n*-butyl	H	0.78	0.084
11i	(Me)$_2$N	H	0.021	0.005
11j	4-methylpiperazine	H	0.009	0.012
11k	morpholine	H	0.012	0.018
11m	piperidine	H	0.012	0.022
11n	pyrrolidine	H	0.012	0.015

^{a} Values correspond to $n = 2$. ^{b} Values correspond to $n = 2$. For assay conditions see Experimental Section.

accommodating the phenacyl group was rather large and promiscuous. Both lipophilic and hydrophilic substituents were tolerated. No preference was seen for either electron-donating or electron-withdrawing substituents on the phenyl ring. Hydrogen bond donating or accepting substituents were also tolerated with no preference for either.

Our modeling studies suggested that these substituents were interacting with substantial parts of the ATP binding pocket and not just protruding out into solvent-exposed space. The dimethylglycinamide analogue **6c** hinted that trisubstituted amines would be good inhibitors with the added advantage of providing compounds with favorable physical properties. The analogues presented in Table 2 further expand this concept. The need for fully substituted glycinamides is clearly demonstrated by analogues **6b**,**f**. A 5−10-fold loss in activity against both CDK2 and CDK4 is seen with these compounds.

The best analogues contain a six-membered saturated ring with an additional nitrogen at the 4-position. Comparing **6e**,**i** indicates the importance of adding the second nitrogen to these analogues. There is a 10-fold increase in potency for both CDK2 and CDK4 by the judicious placement of this second heteroatom. Additional binding energy was achieved by extending hydrogen bond donating groups out from the 4-position of the six-membered ring. Comparing **6e** with the 4-substituted analogues **6j**−**m** shows another source of achieving a 10-fold boost in potency. Combining the two concepts into one molecule (**6n**,**p**) did not give the additive 100-fold increase in potency we hoped for but still allowed us to introduce a highly polar substituent into these molecules, dramatically improving their physical properties.[15]

Because branching α to the amide carbonyl was not tolerated, we envisioned replacing the α-carbon atom with an sp^2 hybridized nitrogen. This would expand the SAR by introducing an additional hydrogen bond donating element into the molecule as well as modulating the

hydrogen bond accepting properties of the amide carbonyl. These analogues would be substantially more rigid and project their substituents in an alternative fashion as compared to the glycinamde series.

Table 3 shows a sampling of several ureas and semicarbazides that were tested against CDK2 and CDK4. The most active urea was the completely unsubstituted analogue **11a**. The addition of two substituents onto the urea core renders this series inactive (**11b**). The activity of the benzyl urea analogue **11c** is completely ruined by the addition of a methyl group as seen in compound **11d**. This drastic change in activity is likely due to a combination of an intolerance of the binding pocket to branching at this position and the loss of the urea's NH hydrogen bond. In general, the urea series produced potent compounds with poor solubility characteristics as compared to the glycinamides.[15]

Examination of the SAR from both the glycinamide and the urea series reveals the structural tolerance of nitrogen atom substitution at both positions α and β to the amide carbonyl. The functional group that we construct from this analysis is a semicarbazide group. Introducing this pharmacophore had a substantial impact on the compound's activity against CDK4 and to a lesser extent against CDK2. Compounds lacking this pharmacophore tend to be 10-fold less potent against CDK4 when compared to CDK2. The two exceptions to this general observation are compounds **6j**,**p**. These two analogues tap some as yet unidentified binding pocket unique to CDK4 by extending hydrogen bond donating groups out from the 4-postion of their piperidine rings.

Table 3 exemplifies how introducing the semicarbazide moiety greatly enhances the CDK4 activity of this series. Three analogues, **11i**−**k**, show a 10-fold increase in activity against CDK4 when compared to their corresponding glycinamide analogues **6c**,**h**,**i**. CDK2 activity is also effected albeit to a lesser extent although **11i** is 10-fold more potent than **6c**. A much larger CDK4 potency increase is seen when comparing **6e** and **11m**.

Table 4. Cellular Activity for Selected Compounds

compd	R	X	HCT116 IC$_{50}$ (μM)^a	PB HCT116 IC$_{50}$ (μM)^b	AG1523 IC$_{50}$ (μM)^b
6j	4-aminomethylpiperazine	CH$_2$	0.07	NM^c	0.6
6k	4-amidopiperidine	CH$_2$	0.04	NM^c	0.4
6p	4-amidinopiperazine	CH$_2$	>0.9	NM^c	NM^c
6n	4-amidopiperazine	CH$_2$	0.047	>5.2	>0.4
11a	H	NH	0.057	3.2	0.413
11e	4-picolyl	NH	0.378	>58	>24
11i	(Me)$_2$N	NH	0.028	1.24	0.385
11k	morpholine	NH	0.020	0.622	0.95
11j	*N*-methylpiperazine	NH	0.015	NM^c	0.085

^{a} Values correspond to $n = 4$. ^{b} Values correspond to $n = 2$. ^{c} NM = not measured. For all assay conditions see Experimental.

Here, the enhancement is greater than 100-fold while the CDK2 activity shows a more modest 5-fold improvement. There does not appear to be an obvious reason for this activity enhancement. A model of **11i** bound to CDK4 shows the ability of the semicarbazide NH to create hydrogen bonds with the side chain carbonyl of Asp 156.[16] This would explain the improved activity profile of the ureas and semicarbazide relative to the glycinamides but fails to explain why this enhancement is so pronounced in the CDK4 activity. This residue is conserved in both kinases and theoretically should provide a similar enhancement against both targets. More detailed structural information (X-ray crystallographic data on a semicarbazide analog) would be required to resolve this issue.

Several of our best compounds were tested against a transformed human colon cancer cell line (HCT116), and those results are summarized in Table 4. The compounds were able to penetrate the cell membrane and have profound effects on the growth and proliferation of this cell line. For comparison, we also screened these compounds against a normal human fibroblast cell line (AG1523) as an indicator of general toxicity. The lack of activity for compound **6p** is probably due to the highly polar nature of the amidine group present in this molecule, preventing the compound from crossing the cell membrane. In general, there appears to be an acceptable margin of toxicity vs the transformed cell line as compared to the normal cell line. In the case of **6n**, this window is greater than 80-fold.

We also measured the effect of serum protein binding on the compounds' ability to inhibit the growth of the same transformed cell line (PB HCT116). Unfortunately, we observed a substantial impact on this series' ability to inhibit cell growth in the presence of serum proteins indicating that these compounds are highly protein bound. One promising analogue **11k** showed a reduced protein binding shift value with an adjusted IC$_{50}$ below 1 μM. This unique morpholine-containing semicarbazide was exploited in subsequent analogues in this series.

Conclusion

We have presented a novel series of indenopyrazole-based CDK inhibitors. Kinetic experiments support our initial molecular modeling studies that the compounds are competitive with ATP and most likely bind in the kinase ATP binding pocket. Molecular modeling studies indicate that the molecules create a similar hydrogen bond donating/accepting network found in many other known small molecule CDK inhibitors for which structural information is available. A unique combination of active pharmacophores led us to a series of semicarbazide-based inhibitors that are highly potent against CDK2 and CDK4 while maintaining selectivity against other serine/threonine kinases.[17] These compounds were active against a transformed human colon cancer cell line (HCT116) while maintaining an acceptable margin of toxicity against a normal fibroblast cell line. The compounds were found to be highly protein bound in our cell-based assay with the exception of **11k**, which maintained a reasonable level of activity in the presence of human plasma proteins.

Experimental Section

All reactions were carried out with continuous stirring under an atmosphere of dry nitrogen. Commercial reagents were used as received without additional purification. Anhydrous solvents were obtained commercially and used without further drying. ^{1}H NMR spectra were obtained using either a Varian (Palo Alto, CA) Unity-300, Inova-300, VXR-400, or Inova-400 spectrometer. Chemical shifts are reported in parts per million relative to tetramethylsilane (TMS) as internal standard. Mass spectra were obtained using either a Finnigan MAT8230 sector or MAT95S sector with an API interface system. Thin-layer chromatography (TLC) was performed on E. Merck 15719 silica gel plates. Flash chromatography was carried out using EM Science silica gel 60 (230−400 mesh). High-performance liquid chromatography (HPLC) purifications were performed on a Rainin Dynamax SD300 instrument using a C18 reverse phase column with acetonitrile/water (containing 0.05% trifluoroacetic acid (TFA)) as a mobile phase. HPLC purity values were obtained using a Rainin Dynamax SD300 instrument system with a photodiode array detector. Melting points were determined in open glass capillaries using a Thomas-Hoover UniMelt melting point apparatus and are uncorrected. Solubility was determined by HPLC analysis of supernatants from a pH 3.5 buffered 5% mannitol solution. Microanalyses were performed by Quantitative Technologies Inc. and were within 0.4% of the calculated values. For compounds where analysis was not obtained, HPLC analysis was used, and purity was determined to be >98%.

2-(4-Methoxybenzoyl)indan-1,3-dione (2). A solution of dimethylphthalate (1 g, 5.2 mmol) and 4-methoxyacetophenone (0.78 g, 5.2 mmol) in dry DMF (3 mL) was heated to 90 °C.

Sodium hydride (0.21 g, 60% suspension in oil, 5.2 mmol) was added in one portion, and the exothermic reaction turned deep red. After 20 min, the reaction was cooled to room temperature, diluted with water (25 mL), and extracted with EtOAc (10 mL) and the aqueous phase was separated. The aqueous phase was acidified to pH 2 with 2 N HCl, and the crude product was collected. Recrystallization with ethanol gave the desired product as a yellow solid (0.4 g, 50%).

3-(4-Methoxyphenyl)-2H-indeno[1,2-c]pyrazol-4-one (1). A solution of 2-(4-methoxybenzoyl)indan-1,3-dione (0.2 g, 0.6 mmol) in EtOH (5 mL) was treated with hydrazine hydrate (0.1 mL, 1.8 mmol) and *p*-TsOH (3 mg). The reaction was heated to reflux and stirred for 2 h. The reaction was cooled to room temperature, and the product was crystallized from the reaction mixture. The product was collected by filtration as a yellow solid (0.1 g, 50%); mp 268 °C. HRMS *m/e* calcd for $C_{19}H_{16}N_3O_3$ (M + H), 334.1192; found, 334.1168. Anal. ($C_{19}H_{15}N_3O_3$) C, H, N.

3-(4-Methoxyphenyl)-2-methyl-2H-indeno[1,2-c]pyrazol-4-one (3a). mp >300 °C. NMR (CDCl₃): δ 8.3 (d, *J* = 8.8 Hz, 2 H), 7.7 (m, 2 H), 7.3 (m, 2 H), 7.0 (d, *J* = 8.8 Hz, 2 H), 4.1 (s, 3 H), 3.9 (s, 3 H). HRMS *m/e* calcd for $C_{18}H_{15}N_2O_2$ (M + H), 291.1134; found, 291.1168. Anal. ($C_{18}H_{14}N_2O_2$) C, H, N.

6-Hydroxy-3-(4-methoxyphenyl)-2H-indeno[1,2-c]pyrazol-4-one (3b). mp >300 °C. NMR (DMSO-d_6): δ 13.6 (bs, 1 H), 8.1 (d, *J* = 7.0 Hz, 1 H), 7.7 (d, *J* = 7.0 Hz, 2 H), 7.4 (d, *J* = 7.0 Hz, 1 H), 7.1 (d, *J* = 7.0 Hz, 1 H), 6.9 (d, *J* = 8.8 Hz, 2 H), 3.8 (s, 3 H). HRMS *m/e* calcd for $C_{17}H_{13}N_2O_3$ (M + H), 293.0926; found, 293.0991. Anal. ($C_{17}H_{12}N_2O_3$) C, H, N.

5-Hydroxy-3-(4-methoxyphenyl)-2H-indeno[1,2-c]pyrazol-4-one (3d). mp >300 °C. NMR (DMSO-d_6): δ 13.4 (bs, 1 H), 8.1 (d, *J* = 8.8 Hz, 2 H), 7.3 (d, *J* = 7.0 Hz, 1 H), 7.1 (d, *J* = 8.8 Hz, 2 H), 6.9 (d, *J* = 7.0 Hz, 1 H), 6.7 (d, *J* = 7.0 Hz, 1 H), 3.8 (s, 3 H). HRMS *m/e* calcd for $C_{17}H_{13}N_2O_3$ (M + H), 293.0926; found, 293.0981. Anal. ($C_{17}H_{12}N_2O_3$) C, H, N.

5-Acetamido-3-(4-methoxyphenyl)-2H-indeno[1,2-c]-pyrazol-4-one (3e). mp >300 °C. NMR (DMSO-d_6): δ 13.1 (bs, 1 H), 8.1 (d, *J* = 8.8 Hz, 2 H), 7.9 (s, 1 H), 7.6 (d, *J* = 7.0 Hz, 1 H), 7.5 (d, *J* = 7.0 Hz, 1 H), 7.4 (d, *J* = 7.0 Hz, 1 H), 7.1 (d, *J* = 8.8 Hz, 2 H), 3.8 (s, 3 H), 2.4 (s, 3 H). HRMS *m/e* calcd for $C_{19}H_{16}N_3O_3$ (M + H), 334.1192; found, 334.1183. Anal. ($C_{19}H_{15}N_3O_3$) C, H, N.

6-Amino-3-(4-methoxyphenyl)-2H-indeno[1,2-c]pyrazol-4-one (3f). mp >300 °C. NMR (DMSO-d_6): δ 13.0 (bs, 1 H), 8.1 (d, *J* = 8.8 Hz, 2 H), 7.2 (d, *J* = 7.7 Hz, 1 H), 7.1 (d, *J* = 8.8 Hz, 2 H), 6.6 (s, 1 H), 6.4 (d, *J* = 7.7 Hz, 1 H), 6.2 (s, 2 H), 3.8 (s, 3 H). HRMS *m/e* calcd for $C_{17}H_{14}N_3O_2$ (M + H), 292.1086; found, 292.1077. Anal. ($C_{17}H_{13}N_3O_2$) C, H, N.

3-(4-Methoxyphenyl)-2-phenyl-2H-indeno[1,2-c]pyrazol-4-one (3g). mp >300 °C. NMR (CDCl₃): δ 8.3 (d, *J* = 8.8 Hz, 2 H), 7.8 (d, *J* = 7.7 Hz, 1 H), 7.6 (m, 4 H), 7.3 (m, 4 H), 7.0 (d, *J* = 8.8 Hz, 2 H), 6.9 (d, *J* = 7.7 Hz, 1 H), 3.8 (s, 3 H). HRMS *m/e* calcd for $C_{23}H_{17}N_2O_2$ (M + H), 353.1290; found, 353.1278. Anal. ($C_{23}H_{16}N_2O_2$) C, H, N.

1-(4-Methoxyphenyl)-2H-2,3,5-triaza-cyclyopenta[a]inden-8-one (3h). mp >300 °C. NMR (DMSO-d_6): δ 13.0 (bs, 1 H), 8.9 (m,1 H), 8.7 (d, *J* = 7.7 Hz, 1 H), 8.2 (d, *J* = 8.8 Hz, 2 H), 7.6 (d, *J* = 7.7 Hz, 1 H), 7.2 (d, *J* = 8.8 Hz, 2 H), 3.8 (s, 3 H). HRMS *m/e* calcd for $C_{16}H_{12}N_3O_2$ (M + H), 278.0930; found, 278.0944. Anal. ($C_{16}H_{11}N_3O_2$) C, H, N.

1-(4-Methoxyphenyl)-2H-2,3-diaza-pentaleno[1,2-b]-naphthalen-10-one (3i). mp >300 °C. NMR (DMSO-d_6): δ 13.7 (bs, 1 H), 8.2 (m, 3 H), 8.0 (m, 3 H), 7.6 (m, 2 H), 7.1 (d, *J* = 8.8 Hz, 2 H), 3.8 (s, 3 H). HRMS *m/e* calcd for $C_{12}H_{15}N_2O_2$ (M + H), 327.1134; found, 327.1111. Anal. ($C_{12}H_{14}N_2O_2$) C, H, N.

1-(4-Methoxyphenyl)-2H-2,3,4-triaza-cyclyopenta[a]inden-8-one (3j). mp >300 °C. NMR (DMSO-d_6): δ 13.2 (bs, 1 H), 8.7 (d, *J* = 5.8 Hz, 1 H), 8.0 (d, *J* = 7.7 Hz, 1 H), 7.7 (d, *J* = 8.8 Hz, 2 H), 7.4 (dd, *J* = 7.8, 5.8 Hz, 1 H), 7.0 (d, *J* = 8.8 Hz, 2 H), 3.8 (s, 3 H). HRMS *m/e* calcd for $C_{16}H_{12}N_3O_2$ (M + H), 278.0930; found, 278.0947. Anal. ($C_{16}H_{11}N_3O_2$) C, H, N.

6,7-Dichloro-3-(4-methoxyphenyl)-2-phenyl-2H-indeno-[1,2-c]pyrazol-4-one (3k). mp >300 °C. NMR (DMSO-d_6): δ 13.2 (bs, 1 H), 8.2 (d, *J* = 8.8 Hz, 2 H), 7.8 (s, 1 H), 7.7 (s, 1 H), 7.1 (d, *J* = 8.8 Hz, 2 H), 3.8 (s, 3 H). HRMS *m/e* calcd for $C_{17}H_{11}N_2O_2Cl_2$ (M + H), 345.0198; found, 345.0176. Anal. ($C_{17}H_{10}N_2O_2Cl_2$) C, H, N.

5-Amino-3-(4-methoxyphenyl)-2-phenyl-2H-indeno[1,2-c]pyrazol-4-one (4). A suspension of **3c** (1.0 g, 3.0 mmol) in MeOH (10 mL) was treated with concentrated HCl (1 mL) and heated to reflux. After the mixture was stirred for 2 h, the reaction was cooled and the product was collected by filtration and obtained as a greenish solid (0.7 g, 80%); mp 273 °C. NMR (DMSO-d_6): δ 13.6 (bs, 1 H), 8.3 (d, *J* = 8.4 Hz, 1 H), 8.1 (d, *J* = 8.8 Hz, 2 H), 7.5 (t, *J* = 7.7 Hz 1 H), 7.2 (d, *J* = 7.0 Hz, 1 H), 7.1 (d, *J* = 8.8 Hz, 2 H), 3.8 (s, 3 H). HRMS *m/e* calcd for $C_{17}H_{14}N_3O_2$ (M + H), 292.1086; found, 292.1080. Anal. ($C_{17}H_{13}N_3O_2$) C, H, N.

2-Chloro-N-[3-(4-methoxyphenyl)-4-oxo-2,4-dihydro-indeno[1,2-c]pyrazol-5-yl]acetamide (5). A suspension of **4** (0.2 g, 0.7 mmol) in acetone (10 mL) was treated with aqueous saturated NaHCO₃ (3 mL) and chloroacetyl chloride (3 mL, 0.21 mmol). The reaction was heated to 50 °C and stirred for 2 h. The reaction was then cooled, poured into water (20 mL), and extracted with EtOAc (100 mL); the organic layer was separated and dried (MgSO₄); and the solvent was removed at reduced pressure. The residue was recrystallized from EtOH to give the product as a yellow solid (0.2 g, 75%); mp >300 °C. NMR (DMSO-d_6): δ 13.6 (bs, 1 H), 11.3 (s, 1 H), 8.3 (d, *J* = 8.4 Hz, 1 H), 8.1 (d, *J* = 8.8 Hz, 2 H), 7.5 (t, *J* = 7.7 Hz 1 H), 7.2 (d, *J* = 7.0 Hz, 1 H), 7.1 (d, *J* = 8.8 Hz, 2 H), 4.5 (s, 2 H), 3.8 (s, 3 H). HRMS *m/e* calcd for $C_{19}H_{15}N_3O_3Cl$ (M + H), 368.0802; found, 368.0818.

3-(4-Methoxyphenyl)-5-(aminoacetamido)indeno[1,2-c]pyrazol-4-one (6b). A suspension of **5** (0.015 g, 0.04 mmol) in EtOH (1 mL) was treated with concentrated NH₄OH (1 mL), placed in a sealed tube, and heated to 80 °C for 3 h. The reaction was cooled, and the solvent was removed at reduced pressure. The residue was recrystallized from EtOH to give the product as a yellow solid (0.009 g, 62%); mp >300 °C. NMR (DMSO-d_6): δ 13.6 (bs, 1 H), 11.3 (s, 1 H), 8.3 (d, *J* = 8.4 Hz, 1 H), 8.1 (d, *J* = 8.8 Hz, 2 H), 7.5 (t, *J* = 7.7 Hz 1 H), 7.2 (d, *J* = 7.0 Hz, 1 H), 7.1 (d, *J* = 8.8 Hz, 2 H), 3.8 (s, 3 H). HRMS *m/e* calcd for $C_{19}H_{17}N_4O_3$ (M + H), 349.1301; found, 349.1309. Anal. ($C_{19}H_{16}N_4O_3$) C, H, N.

3-(4-Methoxyphenyl)-5-(N,N-dimethylaminoacetamido)-indeno[1,2-c]pyrazol-4-one (6c). mp 279 °C. NMR (DMSO-d_6): δ 13.6 (bs, 1 H), 11.3 (s, 1 H), 8.3 (d, *J* = 8.4 Hz, 1 H), 8.1 (d, *J* = 8.8 Hz, 2 H), 7.5 (t, *J* = 7.7 Hz 1 H), 7.2 (d, *J* = 7.0 Hz, 1 H), 7.1 (d, *J* = 8.8 Hz, 2 H), 3.8 (s, 3 H), 3.1 (s, 2 H), 2.3 (s, 6 H). HRMS *m/e* calcd for $C_{21}H_{21}N_4O_3$ (M + H), 377.1614; found, 377.1640. Anal. ($C_{21}H_{20}N_4O_3$) C, H, N.

3-(4-Methoxyphenyl)-5-(piperazinylacetamido)indeno-[1,2-c]pyrazol-4-one (6d). mp 277 °C. NMR (DMSO-d_6): δ 13.6 (bs, 1 H), 11.3 (s, 1 H), 8.35 (d, *J* = 8.4 Hz, 1 H), 8.1 (d, *J* = 8.8 Hz, 2 H), 7.5 (t, *J* = 7.7 Hz 1 H), 7.2 (d, *J* = 7.0 Hz, 1 H), 7.1 (d, *J* = 8.8 Hz, 2 H), 3.3 (bs, 4 H), 3.1 (s, 2 H), 2.8 (bs, 4 H). HRMS *m/e* calcd for $C_{23}H_{24}N_5O_3$ (M + H), 418.1817; found, 418.1899. Anal. ($C_{23}H_{23}N_5O_3$) C, H, N.

3-(4-Methoxyphenyl)-5-(piperidinylacetamido)indeno-[1,2-c]pyrazol-4-one (6e). mp 291 °C. NMR (DMSO-d_6): δ 13.6 (bs, 1 H), 11.3 (s, 1 H), 8.35 (d, *J* = 8.4 Hz, 1 H), 8.1 (d, *J* = 8.8 Hz, 2 H), 7.5 (t, *J* = 7.7 Hz 1 H), 7.2 (d, *J* = 7.0 Hz, 1 H), 7.1 (d, *J* = 8.8 Hz, 2 H), 3.8 (s, 3 H), 3.3 (bs, 4 H), 3.1 (s, 2 H), 2.4 (bs, 4 H), 1.7 (bs, 2 H). HRMS *m/e* calcd for $C_{24}H_{25}N_4O_3$ (M + H), 417.1927; found, 417.1944. Anal. ($C_{24}H_{24}N_4O_3$) C, H, N.

3-(4-Methoxyphenyl)-5-(ethylaminoacetamido)indeno-[1,2-c]pyrazol-4-one (6f). mp 250 °C. NMR (DMSO-d_6): δ 13.6 (bs, 1 H), 11.3 (s, 1 H), 8.35 (d, *J* = 8.4 Hz, 1 H), 8.1 (d, *J* = 8.8 Hz, 2 H), 7.5 (t, *J* = 7.7 Hz 1 H), 7.2 (d, *J* = 7.0 Hz, 1 H), 7.1 (d, *J* = 8.8 Hz, 2 H), 3.8 (s, 3 H), 3.2 (bs, 2 H), 2.5 (q, *J* = 7.0 Hz, 2 H), 1.1 (t, *J* = 7.0 Hz, 3 H). HRMS *m/e* calcd for $C_{21}H_{21}N_4O_3$ (M + H), 377.1614; found, 377.1643. Anal. ($C_{21}H_{20}N_4O_3$) C, H, N.

3-(4-Methoxyphenyl)-5-(thiomorpholinoacetamido)in-deno[1,2-c]pyrazol-4-one (6g). mp 298 °C. NMR (DMSO-

d_6): δ 13.6 (bs, 1 H), 11.3 (s, 1 H), 8.35 (d, J = 8.4 Hz, 1 H), 8.1 (d, J = 8.8 Hz, 2 H), 7.5 (t, J = 7.7 Hz 1 H), 7.2 (d, J = 7.0 Hz, 1 H), 7.1 (d, J = 8.8 Hz, 2 H), 3.8 (s, 3 H), 3.2 (bs, 2 H), 2.8 (bs, 8 H). HRMS *m/e* calcd for $C_{23}H_{23}N_4O_3S$ (M + H), 435.1491; found, 435.1477. Anal. ($C_{23}H_{22}N_4O_3S$) C, H, N.

3-(4-Methoxyphenyl)-5-(morpholinoacetamido)indeno-[1,2-c]pyrazol-4-one (6h). mp 295 °C. NMR (DMSO-d_6): δ 13.6 (bs, 1 H), 11.3 (s, 1 H), 8.35 (d, J = 8.4 Hz, 1 H), 8.1 (d, J = 8.8 Hz, 2 H), 7.5 (t, J = 7.7 Hz 1 H), 7.2 (d, J = 7.0 Hz, 1 H), 7.1 (d, J = 8.8 Hz, 2 H), 3.8 (s, 3 H), 3.7 (m, 4 H), 3.2 (s, 2 H), 2.6 (m, 4 H). HRMS *m/e* calcd for $C_{23}H_{23}N_4O_4$ (M + H), 419.1719; found, 419.1709. Anal. ($C_{23}H_{22}N_4O_4$) C, H, N.

3-(4-Methoxyphenyl)-5-(4-methylpiperazinylacetami-do)indeno[1,2-c]pyrazol-4-one (6i). mp >300 °C. NMR (DMSO-d_6): δ 13.6 (bs, 1 H), 11.3 (s, 1 H), 8.35 (d, J = 8.4 Hz, 1 H), 8.1 (d, J = 8.8 Hz, 2 H), 7.5 (t, J = 7.7 Hz 1 H), 7.2 (d, J = 7.0 Hz, 1 H), 7.1 (d, J = 8.8 Hz, 2 H), 3.8 (s, 3 H), 3.3 (bs, 4 H), 3.1 (s, 2 H), 2.8 (bs, 4 H), 2.2 (s, 3 H). HRMS *m/e* calcd for $C_{24}H_{26}N_5O_3$ (M + H), 432.2036; found, 432.2030. Anal. ($C_{24}H_{25}N_5O_3$) C, H, N.

3-(4-Methoxyphenyl)-5-(4-aminomethylpiperidinyl-acetamido)indeno[1,2-c]pyrazol-4-one (6j). mp >300 °C. NMR (DMSO-d_6): δ 13.6 (bs, 1 H), 11.3 (s, 1 H), 8.35 (d, J = 8.4 Hz, 1 H), 8.1 (d, J = 8.8 Hz, 2 H), 7.5 (t, J = 7.7 Hz 1 H), 7.2 (d, J = 7.0 Hz, 1 H), 7.1 (d, J = 8.8 Hz, 2 H), 3.8 (s, 3 H), 3.2 (bs, 2 H), 2.9(bs, 2 H), 2.5 (d, J = 8.0 Hz, 2 H), 2.2 (t, J = 8.0 Hz, 2 H), 1.6 (m, 5 H). HRMS *m/e* calcd for $C_{25}H_{28}N_5O_3$ (M + H), 446.2192; found, 446.2169. Anal. ($C_{25}H_{27}N_5O_3$) C, H, N.

3-(4-Methoxyphenyl)-5-(4-amidopiperidinylacetamido)indeno[1,2-c]pyrazol-4-one (6k). mp >300 °C. NMR (DMSO-d_6): δ 13.6 (bs, 1 H), 11.7 (s, 1 H), 8.35 (d, J = 8.4 Hz, 1 H), 8.1 (d, J = 8.8 Hz, 2 H), 7.5 (t, J = 7.7 Hz 1 H), 7.2 (d, J = 7.0 Hz, 1 H), 7.1 (d, J = 8.8 Hz, 2 H), 6.8 (bs, 2 H), 3.8 (s, 3 H), 3.2 (s, 2 H), 2.9 (m, 2 H), 2.2 (m, 2 H), 1.7 (m, 2 H). HRMS *m/e* calcd for $C_{25}H_{26}N_5O_4$ (M + H), 460.1984; found, 460.1997. Anal. ($C_{25}H_{25}N_5O_4$) C, H, N.

3-(4-Methoxyphenyl)-5-(4-hydroxymethylpiperidinyl-acetamido)indeno[1,2-c]pyrazol-4-one (6m). mp >300 °C. NMR (DMSO-d_6): δ 13.6 (bs, 1 H), 11.7 (s, 1 H), 8.35 (d, J = 8.4 Hz, 1 H), 8.1 (d, J = 8.8 Hz, 2 H), 7.5 (t, J = 7.7 Hz 1 H), 7.2 (d, J = 7.0 Hz, 1 H), 7.1 (d, J = 8.8 Hz, 2 H), 4.5 (t, J = 5.5 Hz, 1 H), 3.8 (s, 3 H), 3.4 (m, 2 H), 3.2 (s, 2 H), 2.9 (m, 2 H), 2.2 (m, 2 H), 1.6 (m, 5 H). HRMS *m/e* calcd for $C_{25}H_{27}N_4O_4$ (M + H), 447.2032; found, 447.2012. Anal. ($C_{25}H_{26}N_4O_4$) C, H, N.

3-(4-Methoxyphenyl)-5-(4-amidopiperizinylacetami-do)indeno[1,2-c]pyrazol-4-one (6n). mp >300 °C. NMR (DMSO-d_6): δ 13.6 (bs, 1 H), 11.4 (s, 1 H), 8.35 (d, J = 8.4 Hz, 1 H), 8.1 (d, J = 8.8 Hz, 2 H), 7.5 (t, J = 7.7 Hz 1 H), 7.2 (d, J = 7.0 Hz, 1 H), 7.1 (d, J = 8.8 Hz, 2 H), 6.0 (bs, 2 H), 3.8 (s, 3 H), 3.4 (m, 2 H), 3.2 (s, 2 H). HRMS *m/e* calcd for $C_{24}H_{25}N_6O_4$ (M + H), 461.1937; found, 461.1945. Anal. ($C_{24}H_{24}N_6O_4$) C, H, N.

3-(4-Methoxyphenyl)-5-(4-carbamidoylpiperizinyl-acetamido)indeno[1,2-c]pyrazol-4-one (6p). mp >300 °C. NMR (DMSO-d_6): δ 13.6 (bs, 1 H), 11.5 (s, 1 H), 8.35 (d, J = 8.4 Hz, 1 H), 8.1 (d, J = 8.8 Hz, 2 H), 7.6 (bs, 3 H), 7.2 (d, J = 7.0 Hz, 1 H), 7.1 (d, J = 8.8 Hz, 2 H), 3.8 (s, 3 H), 3.6 (bs, 4 H), 3.2 (s, 2 H), 2.6 (bs, 4 H). HRMS *m/e* calcd for $C_{24}H_{26}N_7O_3$ (M + H), 460.2097; found, 460.2089. Anal. ($C_{24}H_{25}N_7O_3$) C, H, N.

4-Amino-2-(4-methoxy-benzoyl)indan-1,3-dione (8). Compound **7** (2.0 g, 5.93 mmol) was dissolved in 20% HCl in methanol (50 mL). This solution was stirred at reflux for a period of 3 h. It was then allowed to cool to room temperature and stirred overnight. The product was filtered off, washed with ethanol (20 mL), and air-dried to give the product as a yellow solid (1.5 g, 86%); mp 268−269 °C. ^{1}H NMR (DMSO-d_6): δ 8.2 (d, J = 8.8 Hz, 2H), 7.5 (t, 1H), 7.1 (d, J = 8.7 Hz, 2H), 7.0 (m, 2H), 3.9 (s, 1H). HRMS calcd for $C_{17}H_{14}N_1O_4$ (M + H$^+$), 296.0923; found, 296.0899.

[2-(4-Methoxybenzoyl)-1,3-dioxo-indan-4-yl]carbam-ic Acid Phenyl Ester (9). Aniline **8** (1.5 g, 5.08 mmol) was dissolved in acetone (40 mL) and treated with sodium carbonate (1.26 g, 15.24 mmol) and phenyl chloroformate (1.19 g, 7.62 mmol). The suspension was stirred at 50 °C for 3 h. The

reaction mixture was diluted with water (120 mL) and extracted with ethyl acetate (2 × 100 mL). The organic layer was separated, washed with brine (50 mL), and dried (Na$_2$-SO$_4$), and the solvent was removed at reduced pressure to give a gummy orange residue. Cold ethyl ether (100 mL) was added to this residue to give a precipitate. The precipitate was collected and washed with ethyl ether (2 × 10 mL) to give desired product as a yellow solid (1.65 g, 78%); mp 256−58 °C. ^{1}H NMR (DMSO-d_6): δ 10.8 (s, 1H), 8.1 (d, J = 8.0 Hz, 1H), 7.6 (d, J = 2.9 Hz, 2H), 7.5 (m, 3H), 7.3 (m, 3H), 7.1 (t, 1H), 6.9 (d, J = 10.8 Hz, 2H), 3.8 (s, 3H). HRMS calcd for $C_{24}H_{18}N_1O_6$ (M + H$^+$), 416.1134; found, 416.1105.

3-(4-Methoxyphenyl)-5-(butylcarbamoyl)aminoindeno-[1,2-c]pyrazol-4-one (11h). Carbamate **9** (0.03 g, 0.072 mmol) in anhydrous DMSO (2 mL) was treated with butylamine (0.01 g, 0.082 mmol) and 4-(dimethylamino)pyridine (0.005 g, 0.04 mmol) and heated to 80 °C for 3 h. The solvent was removed under reduced pressure, and the residue was triturated with ethanol to give a dark solid. The solid was collected and washed with ethanol (5 mL) to give urea **10** (0.03 g, 100%). The tricarbonyl urea intermediate **10** (0.03 g, 0.078 mmol) was treated with hydrazine hydrate (0.1 mL, 3.21 mmol) and *p*-toluenesulfonic acid monohydrate (0.01 g, 0.05 mmol) in refluxing ethanol (4 mL) for a period of 3 h. The reaction mixture was cooled to room temperature, and the solid was collected, washed with cold ethanol (2 × 2 mL), and air-dried to give the product as a yellowish solid (0.01 g, 30.6%); mp 255−256 °C. ^{1}H NMR (DMSO-d_6): δ 9.41 (s, 1 H), 8.16 (d, J = 8.0 Hz, 2 H), 7.4 (d, J = 6.0 Hz, 1 H), 7.06 (d, J = 9.2 Hz, 2 H), 6.95 (d, J = 7.1 Hz, 1 H), 3.79 (s, 3 H), 2.99 (m, 2 H), 1.43 (m, 2 H), 0.86 (m, 3 H). HRMS calcd for $C_{21}H_{21}N_4O_3$ (M + H$^+$), 377.1614; found, 377.1588. Anal. ($C_{21}H_{20}N_4O_3$) C, H, N.

3-(4-Methoxyphenyl)-5-(carbamoyl)aminoindeno[1,2-c]pyrazol-4-one (11a). mp 267−269 °C. ^{1}H NMR (DMSO-d_6): δ 9.35 (s, 1 H), 8.2 (m, 3 H), 7.4 (m, 1 H), 7.1 (d, J = 8.8 Hz, 2 H), 7.0 (d, J = 7 Hz, 1 H), 3.8 (s, 3 H). HRMS calcd for $C_{18}H_{145}N_4O_3$ (M − H$^-$), 335.1144; found, 335.1162. Anal. ($C_{18}H_{14}N_4O_3$) C, H, N.

3-(4-Methoxyphenyl)-5-(diethylcarbamoyl)aminoinde-no[1,2-c]pyrazol-4-one (11b). mp 261−262 °C. ^{1}H NMR (DMSO-d_6): δ 8.2 (d, J = 8.5 Hz, 1 H), 8.15 (d, J = 9.0 Hz, 1 H), 7.4 (d, J = 8.1 Hz, 2 H), 7.1 (m, 3 H), 3.8 (s, 3 H), 2.9 (m, 4 H), 1.1 (m, 6 H). HRMS calcd for $C_{22}H_{23}N_4O_3$ (M + H$^+$), 391.1770; found, 391.1764. Anal. ($C_{22}H_{22}N_4O_3$) C, H, N.

3-(4-Methoxyphenyl)-5-(benzylcarbamoyl)aminoindeno-[1,2-c]pyrazol-4-one (11c). mp 279−280 °C. ^{1}H NMR (DMSO-d_6): δ 9.5 (s, 1 H), 8.2 (m, 3 H), 7.3 (m, 6 H), 7.1 (m, 3 H), 4.3 (d, J = 5.9 Hz, 2 H), 3.8 (s, 3 H). HRMS calcd for $C_{25}H_{21}N_4O_3$ (M + H$^+$), 425.1614; found, 425.1639. Anal. ($C_{25}H_{20}N_4O_3$) C, H, N.

3-(4-Methoxyphenyl)-5-(1-benzyl-1-methylcarbamoyl)-aminoindeno[1,2-c]pyrazol-4-one (11d). mp 259−260 °C. ^{1}H NMR (DMSO-d_6): δ 9.7 (s, 1 H), 8.3 (d, J = 8.4 Hz, 1 H), 8.1 (d, J = 8.8 Hz, 2 H), 7.4 (m, 1 H), 7.3 (m, 5 H), 7.1 (m, 3 H), 4.6 (s, 2 H), 3.8 (s, 3 H), 3.0 (s, 3 H). HRMS calcd for $C_{26}H_{23}N_4O_3$ (M + H$^+$), 439.1770; found, 439.1762. Anal. ($C_{26}H_{22}N_4O_3$) C, H, N.

3-(4-Methoxyphenyl)-5-(4-picolylcarbamoyl)aminoin-deno[1,2-c]pyrazol-4-one (11e). mp >300 °C. ^{1}H NMR (DMSO-d_6): δ 13.6 (s, 1 H), 9.6 (s, 1 H), 8.5 (d, J = 5.9 Hz, 2 H), 8.3 (m, 1 H), 8.2 (m, 3 H), 7.4 (m, 1 H), 7.3 (d, J = 5.5 Hz, 2 H), 7.10 (m, 3 H), 4.3 (d, J = 5.9 Hz, 2 H), 3.8 (s, 3 H). HRMS calcd for $C_{24}H_{20}N_5O_3$ (M + H$^+$), 426.1566; found, 426.1572. Anal. ($C_{24}H_{19}N_5O_3$) C, H, N.

3-(4-Methoxyphenyl)-5-(4-methoxybenzylcarbamoyl)-aminoindeno[1,2-c]pyrazol-4-one (11f). mp 259−262 °C. ^{1}H NMR (DMSO-d_6): δ 9.4 (s, 1 H), 8.2 (m, 3 H), 7.4 (m, 1 H), 7.2 (m, 2 H), 7.1 (m, 3 H), 6.9 (m, 3 H), 4.2 (d, J = 5.1 Hz, 2 H), 3.8 (s, 3 H), 3.7 (s, 3 H). HRMS calcd for $C_{26}H_{23}N_4O_4$ (M + H$^+$), 455.1719; found, 455.1719. Anal. ($C_{26}H_{22}N_4O_4$) C, H, N.

3-(4-Methoxyphenyl)-5-(phenylcarbamoyl)aminoinde-no[1,2-c]pyrazol-4-one (11g). mp >300 °C. ^{1}H NMR (DMSO-d_6): δ 10.0 (s, 1 H), 9.7 (s, 1 H), 8.2 (m, 3 H), 7.5 (d, J = 7.7 Hz, 2 H), 7.4 (t, 1 H), 7.3 (t, 2 H), 7.1 (m, 3 H), 7.0 (t, 1H), 3.8

(s, 3 H). HRMS calcd for $C_{24}H_{19}N_4O_3$ (M + H$^+$), 411.1457; found, 411.1478. Anal. ($C_{24}H_{18}N_4O_3$) C, H, N.

3-(4-Methoxyphenyl)-5-(dimethylaminocarbamoyl)-aminoindeno[1,2-c]pyrazol-4-one (11i). mp 258−259 °C. ^{1}H NMR (DMSO-d_6): δ 8.3 (d, J = 8.8 Hz, 1 H), 8.1 (d, J = 8.8 Hz, 2 H), 8.0 (s, 1 H), 7.4 (m, 1 H), 7.1 (d, J = 8.8 Hz, 2 H), 7.1 (d, J = 6.9 Hz, 1 H), 3.8 (s, 3 H), 2.6 (s, 6 H). HRMS calcd for $C_{20}H_{20}N_5O_3$ (M + H$^+$), 378.1566; found, 378.1579. Anal. ($C_{20}H_{19}N_5O_3$) C, H, N.

3-(4-Methoxyphenyl)-5-(4-methylpiperazinylcarbamoyl)aminoindeno[1,2-c]pyrazol-4-one (11j). mp >300 °C. NMR (DMSO-d_6): δ 13.6 (bs, 1 H), 11.3 (s, 1 H), 8.35 (d, J = 8.4 Hz, 1 H), 8.1 (d, J = 8.8 Hz, 2 H), 7.5 (t, J = 7.7 Hz 1 H), 7.2 (d, J = 7.0 Hz, 1 H), 7.1 (d, J = 8.8 Hz, 2 H), 3.8 (s, 3 H), 3.3 (bs, 4 H), 2.8 (bs, 4 H), 2.2 (s, 3 H). HRMS m/e calcd for $C_{23}H_{25}N_6O_3$ (M + H), 433.1987; found, 433.1990. Anal. ($C_{23}H_{24}N_6O_3$) C, H, N.

3-(4-Methoxyphenyl)-5-(morpholinylcarbamoyl)aminoindeno[1,2-c]pyrazol-4-one (11k). mp 290−291 °C. ^{1}H NMR (DMSO-d_6): δ 8.3 (d, J = 6.8 Hz, 2 H), 8.2 (d, J = 8.8 Hz, 2 H), 7.4 (m, 1 H), 7.1 (m, 3 H), 3.8 (s, 3 H), 2.9 (m, 4 H), 2.7 (m, 4 H). HRMS calcd for $C_{22}H_{22}N_5O_4$ (M + H$^+$), 420.1672; found, 420.1688. Anal. ($C_{22}H_{21}N_5O_4$) C, H, N.

3-(4-Methoxyphenyl)-5-(piperidinylcarbamoyl)aminoindeno[1,2-c]pyrazol-4-one (11m). mp >300 °C. NMR (DMSO-d_6): δ 13.6 (bs, 1 H), 11.3 (s, 1 H), 8.35 (d, J = 8.4 Hz, 1 H), 8.1 (d, J = 8.8 Hz, 2 H), 7.5 (t, J = 7.7 Hz 1 H), 7.2 (d, J = 7.0 Hz, 1 H), 7.1 (d, J = 8.8 Hz, 2 H), 3.8 (s, 3 H), 3.3 (bs, 4 H), 1.7 (bs, 2 H). HRMS m/e calcd for $C_{23}H_{24}N_5O_3$ (M + H), 418.1879; found, 418.1868. Anal. ($C_{23}H_{23}N_5O_3$) C, H, N.

3-(4-Methoxyphenyl)-5-(pyrrolidinylcarbamoyl)aminoindeno[1,2-c]pyrazol-4-one (11n). mp 291−293 °C. NMR (DMSO-d_6): δ 13.6 (bs, 1 H), 11.3 (s, 1 H), 8.35 (d, J = 8.4 Hz, 1 H), 8.1 (d, J = 8.8 Hz, 2 H), 7.5 (t, J = 7.7 Hz 1 H), 7.2 (d, J = 7.0 Hz, 1 H), 7.1 (d, J = 8.8 Hz, 2 H), 3.8 (s, 3 H), 3.3 (bs, 4 H), 2.4 (bs, 4 H). HRMS m/e calcd for $C_{22}H_{22}N_5O_3$ (M + H), 404.1723; found, 404.1739. Anal. ($C_{22}H_{21}N_5O_3$) C, H, N.

Molecular Modeling. A homology model was generated for CDK4 based on the crystallographic structure of CDK2 complexed with cyclin A and ATP (PDB entry 1FIN).[18] The Modeler program[19] (MSI, San Diego, CA) was used to generate 25 models of the cyclin-bound conformation of CDK4. The WHAT IF program[20] was used to select the best model. Compounds were then docked into the ATP active site using InsightII v97.0 (MSI). The protein was held rigid, while the flexible inhibitor was minimized in the active site using the CFF97 force field (MSI). Compounds were hand-docked into the active site in multiple orientations until a satisfactory binding mode was determined.

Kinetic Analysis. Kinase assays were performed at 23 °C for 15 min with GST-Rb at 3 μM. Initial velocity studies for IC$_{50}$ determinations were performed at varying inhibitor concentration and at different fixed concentrations of ATP as indicated. Rates are recorded as pmol of phosphate transferred to GST-Rb per minute per pmol of enzyme. IC$_{50}$ data were fit to eq 1 using the program Kaleidagraph.

$$(v/v_o) \times 100 = 100/(1 + [I]/IC_{50})^f \quad (1)$$

where f = slope.

CDK2/E Enzyme Inhibition. CDK2/his-cyclinE was prepared as previously described.[21] CDK2/cyclinE kinase reactions were carried out in 50 μL reactions containing 50 mM Tris-HCl (pH 7.6), 10 mM MgCl$_2$, 10% DMSO, 1 mM dithiothreitol, 50 μM ATP, 0.05 μCi [γ-^{32}P]ATP (2000 Ci/mmol, NEN Life Science Products), and 6 μM GST-Rb fusion. After they were incubated at room temperature, the reactions were terminated by addition of an equal volume of cold phosphate-buffered saline (PBS) containing 100 mM ethylenediaminetetraacetic acid (EDTA), 10 mM ATP, 200 μg/mL bovine serum albumin (BSA), and 0.2% NP40. Aliquots of the stopped reactions were processed as described previously.[22]

CDK4/D1 Enzyme Inhibition. CDK4/D1 complexes were expressed in insect cells following dual infection by baculovirus

vectors containing each of the components, and extracts of these cells were then prepared as described previously.[23] CDK4/D1 kinase activity was measured in 96 well polypropylene microtiter plates using a GST-60 kDa Rb fusion protein (comprising amino acids 378 to 928 of Rb) and γ-^{32}P-ATP and capturing the ^{32}P-labeled reaction products on GSH-Sepharose beads.[24] Briefly, each reaction (50 μL) contained 50 mM Tris-HCl (pH 7.6), 10 mM MgCl$_2$, 10% DMSO, 1 mM DTT, 50 μM ATP, 10 μg/mL BSA, 1% glycerol, 6 μg GST-Rb (60 kDa Rb), and 0.5 μCi [γ-^{32}P]ATP. Kinase reactions were initiated by addition of 4 units of CDK4/D1. One unit of CDK4/D1 kinase activity results in the transfer of 1 pmol of ^{32}P per minute at room temperature to the GST-Rb fusion protein. After 15 min, 50 μL of stop buffer (PBS with 100 mM Na$_2$EDTA, 10 mM ATP, 200 μg/mL BSA, and 0.2% NP-40) was added to the reaction. Half of the reaction was then transferred to a Millipore MHVB N45 filter plate containing 50 μL of GSH-Sepharose beads (25% slurry in PBS with 0.8% NP40 and 80 mM Na$_2$EDTA) to capture the GST-Rb. The plates were incubated at room temperature for 90 min with continuous mixing on a plate shaker. After they were filtered, each well was washed 5 times with 200 μL of PBS containing 0.5% NP-40. The samples were dried, and 50 μL of Microscint scintillation fluid was added to each well. The ^{32}P radioactivity in each sample was determined using the Packard Top Count scintillation counter. In a typical experiment, less than 10% of the GST-Rb was phosphorylated and greater than 95% of the radioactivity was found in Rb by sodium dodecyl sulfate polyacrylamide gel electrophoresis analysis.

Cellular Growth Inhibition Assays. Effects of compounds on growth of a human colon carcinoma cell line (HCT116; ATCC) and normal human fibroblasts (AG1523; Coriell Institute for Medical Research) were evaluated in a colorimetric assay using sulforhodamine B (SRB).[25] Briefly, exponentially growing cells were seeded in wells of a 96 well microtiter plate containing McCoys5A media and 5% fetal bovine serum (FBS) at a concentration to allow for 3−5 doublings before obtaining 85% confluence. Eighteen hours later, graded concentrations of test compounds were added to the cell plates. Plates were incubated for 5 (HCT-116) or 6 (AG1523) days at 37 °C in 5% CO$_2$. A 50 μL amount of cold 50% TCA was gently added to each well, and plates were placed at 4 °C for 1 h. Plates were decanted, rinsed 5 times with cold tap water, and allowed to air dry. A 50 μL amount of 0.4% SRB in 1% acetic acid was added, and the plates were incubated at room temperature for 15 min. Plates were washed 4 times with 1% acetic acid and again allowed to air dry. A 150 μL amount of 10 mM Tris base was added, and plates were agitated on a plate shaker for 5 min before reading optical densities at 570 nm using a BIORAD 3550 plate reader.

Protein Binding Assay. The effect of human serum protein binding on inhibition of growth was determined by the addition of 45 mg/mL human serum albumin (Cat. no. A-3782, Sigma Chemicals) and 1 mg/mL α-1-acid-glycoprotein (Cat. no. G-9885, Sigma Chemicals) simultaneously with compound to HCT116 cells. Growth and assay conditions were as described above with 3-(4,5-dimethylthiazol-2-yl)-2,5-diphenyltetrazolium bromide (MTT) used as an indicator of metabolic activity to determine growth inhibition. Briefly, 100 μL of growth medium was removed at the end of the compound incubation period and 50 μL of a 1 mg/mL solution of MTT was added. The cell plates were incubated for 4 h at 37 °C, 5% CO$_2$. A 200 μL amount of 0.04 N HCl in isopropyl alcohol was added, and cultures were vigorously mixed to solubilize resultant purple formizan precipitate. Absorbances were read in a BIORAD 3550 Microplate Reader at a test wavelength of 570 nm and a reference wavelength of 630 nm.

References

(1) Pardee, A. B. G1 Events and Regulation of Cell Proliferation. *Science* **1989**, *246*, 603−608.

(2) Meijer, L.; Guidet, S.; Philippe, M. *Progress in Cell Cycle Research*; Plenum: New York, 1997; Vol. 3.

(3) (a) Draetta, G.; Pagano, M. Cell Cycle Control and Cancer. *Annu. Rep. Med. Chem.* **1996**, *31*, 241−248. (b) Hartwell, L. H.; Kastan, M. B. Cell Cycle Control and Cancer. *Science* **1994**, *266*, 1821−1828. (c) Hunter, T.; Pines, J. Cyclins and Cancer II: Cyclin D and CDK Inhibitors Come of Age. *Cell* **1994**, *79*, 573−582.

(4) (a) Toogood, P. L. Cyclin-dependent kinase inhibitors for treating cancer. *Med. Res. Rev.* **2001**, *21* (6), 487−498. (b) Fischer, P. M. Recent advances and new directions in the discovery and development of cyclin-dependent kinase inhibitors. *Curr. Opin. Drug Discovery Dev.* **2001**, *4* (5), 623−634. (c) Meijer, L. Cyclin-dependent kinases inhibitors as potential anticancer, antineurodegenerative, antiviral and antiparasitic agents. *Drug Resist. Updates* **2000**, *3* (2), 83−88. (d) Sielecki, T. M.; Boylan, J. F.; Benfield, P. A.; Trainor, G. L. Cyclin-Dependent Kinase Inhibitors: Useful Targets in Cell Cycle Regulation. *J. Med. Chem.* **2000**, *43* (1), 1.

(5) (a) Vesely, J.; Havlicek, L.; Strnad, M.; Blow, J. J.; Donella-Deana, A.; Pinna, L.; Letham, D. S.; Kato, J.-Y.; Detivaud, L.; Leclerc, S.; Meijer, L. Inhibition of Cyclin-Dependent Kinases by Purine Analogues. *Eur. J. Biochem.* **1994**, *224*, 771−786. (b) Gray, N. S.; Wodicka, L.; Thunnissen, A.-M.; Norman, T. C.; Kwon, S.; Espinoza, F. H.; Morgan, D. O.; Barnes, G.; Leclerc, S.; Meijer, L.; Kim, S.-H.; Lockhart, D. J.; Schultz, P. G. Exploiting Chemical Libraries, Structure, and Genomics in the Search of Kinase Inhibitors. *Science* **1998**, *281*, 533−538. (c) Schultz, C.; Link, A.; Leost, M.; Zaharevitz, D. W.; Gussio, R.; Sausville, E. A.; Meijer, L.; Kunick, C. Paullones, a Series of Cyclin-Dependent Kinase Inhibitors: Synthesis, Evaluation of CDK1/Cyclin B Inhibition, and in Vitro Antitumor Activity. *J. Med. Chem.* **1999**, *42* (23), 2909−2919. (d) Barvian, M.; Boschelli, D. H.; Cossrow, J.; Dobrusin, E.; Fattaey, A.; Fritsch, A.; Fry, D.; Harvey, P.; Keller, P.; Garrett, M.; La, F.; Leopold, W.; McNamara, D.; Quin, M.; Trumpp-Kallmeyer, S.; Toogood, P.; Wu, Z.; Zhang, E. Pyrido[2,3-d]pyrimidin-7-one Inhibitors of Cyclin-Dependent Kinases. *J. Med. Chem.* **2000**, *43* (24), 4606−4616. (e) Arris, C. E.; Boyle, F. T.; Calvert, A. H.; Curtin, N. J.; Endicott, J. A.; Garman, E. F.; Gibson, A. E.; Golding, B. T.; Grant, S.; Griffin, R. J.; Jewsbury, P.; Johnson, L. N.; Lawrie, A. M.; Ne, D. R. Identification of Novel Purine and Pyrimidine Cyclin-Dependent Kinase Inhibitors with Distinct Molecular Interactions and Tumor Cell Growth Inhibition Profiles. *J. Med. Chem.* **2000**, *43* (15), 2797−2804.

(6) (a) Sedlacek, H. H.; Czech, J.; Naik, R.; Kaur, G.; Worland, P.; Losiewicz, M.; Parker, B.; Carlson, B.; Smith, A.; Senderowicz, A.; Sausville, E. Flavopiridol (L86-8275, NSC-649890), a New Kinase Inhibitor for Tumor Therapy. *Int. J. Oncol.* **1996**, *9*, 1143−1168. (b) Senderowicz, A. M.; Headlee, D.; Stinson, S. F.; Lush, R. M.; Kalil, N.; Villalba, L.; Hill, K.; Steinberg, S. M.; Figg, W. D.; Tompkins, A.; Arbuck, S. G.; Sausville, E. A. Phase I Trial of Continuous Infusion Flavopiridol, a Novel Cyclin-Dependent Kinase Inhibitor, in Patients with Refractory Neoplasms. *J. Clin. Oncol.* **1998**, *16*, 2986−2999. (c) Akinaga, S.; Sugiyama, K.; Akiyama, T. UCN-01 (7-hydroxystaurosporine) and other indolocarbazole compounds: a new generation of anticancer agents for the new century? *Anti-Cancer Drug Des.* **2000**, *15* (1), 43−52.

(7) Nugiel, D. A.; Etzkorn, A. M.; Vidwans, A.; Benfield, P. A.; Boisclair, M.; Burton, C. R.; Cox, S.; Czerniak, P. M.; Doleniak, D.; Seitz, S. P Indenopyrazoles as Novel Cyclin Dependent Kinase (CDK) Inhibitors. *J. Med. Chem.* **2001**, *44*, 1334−1336. Part 1 in this series.

(8) Yue, E. W.; Higley, C. A.; DiMeo, S. V.; Carini, D. J.; Nugiel, D. A.; Benware, C.; Benfield, P. A.; Burton, C. R.; Cox, S.; Grafstrom, R. H.; Boylan, J. F.; Muckelbauer, J. K.; Smallwood, A. M.; Chen, H.; Chang, C.-H.; Seitz, S. P.; Trainor, G. L. Synthesis and Evaluation of Indenopyrazoles as Cyclin-Dependent Kinase Inhibitors. 3. Structure Activity Relationships at C3. *J. Med. Chem.* **2002**, *45*, 5233−5248.

(9) Kilgore, L. B.; Ford, J. H.; Wolfe, W. C. Insecticidal Properties of 1,3-Indandiones *Ind. Eng. Chem.* **1942**, *34* (4), 494−497.

(10) Activity against c-Abl was measured for **3b,d** and found to be 6.5 and 25 μM, respectively.

(11) (a) Dreyer, M. K.; Borcherding, D. R.; Dumont, J. A.; Peet, N. P.; Tsay, J. T.; Wright, P. S.; Bitonti, A. J.; Shen, J.; Kim, S.-H. Crystal Structure of Human Cyclin-Dependent Kinase 2 in Complex with the Adenine-Derived Inhibitor H717. *J. Med. Chem.* **2001**, *44* (4), 524−530. (b) De Bondt, H. L.; Rosenblatt, J.; Jancarik, J.; Jones, H. D.; Morgan, D. O.; Kim, S.-H. Crystal structure of cyclin-dependent kinase 2. *Nature* **1993**, *363*, 595−602. (c) Lawrie, A. M.; Noble, M. E. M.; Tunnah, P.; Brown, N. R.; Johnson, L. N.; Endicott, J. A. Protein kinase inhibition by staurosporine revealed in details of the molecular interaction with CDK2. *Nat. Struct. Biol.* **1997**, *4*, 796−801. (d) De Azevedo, W. F.; Mueller-Dieckmann, H.-J.; Schulze-Gahmen, U.; Worland, P. J.; Sausville, E.; Kim, S.-H. Structural basis for specificity and potency of a flavonoid inhibitor of human CDK2, a cell cycle kinase. *Proc. Natl. Acad. Sci. U.S.A.* **1996**, *93*, 2735−2740.

(12) (a) Jeffrey, P. D.; Russo, A. A.; Polyak, K.; Gibbs, E.; Hurwitz, J.; Massague, J.; Pavletich, N. P. Mechanism of CDK activation revealed by the structure of a cyclinA-CDK2 complex. *Nature* **1995**, *376*, 313−320. (b) Russo, A. A.; Jeffrey, P. D.; Patten, A. K.; Massague, J.; Pavletich, N. P. Crystal structure of the p27 Kip1 cyclin-dependent kinase inhibitor bound to the cyclin A-CDK2 complex. *Nature* **1996**, *382*, 325−331.

(13) Ducrot, P.; Legraverend, M.; Grierson, D. S. 3D-QSAR CoMFA on Cyclin-Dependent Kinase Inhibitors. *J. Med. Chem.* **2000**, *43*, 4098−4108.

(14) Schulze-Gahmen, U.; Brandsen, J.; Jones, H. D.; Morgan, D. O.; Meijer, L.; Vesely, J.; Kim, S.-H. Multiple modes of ligand recognition: Crystal structures of cyclin-dependent protein kinase 2 in complex with ATP and two inhibitors, olomoucine and isopentenyladenine. *Proteins: Struct., Funct., Genet.* **1995**, *22*, 378−391.

(15) Solubility for indenopyrazole analogues was determined using a buffered 5% mannitol solution with a pH of 3.5; **6a** = 0.01 mg/mL; **6c** = 0.72 mg/mL; **6j** = 0.43 mg/mL; **6p** = 0.38 mg/mL; **11a** = <0.001 mg/mL.

(16) A model of **11i** bound in the ATP binding pocket of CDK4 shows the molecule overlapping with **3c** in an identical orientation except for the additional atoms that make up the semicarbazide moiety. The proximity of Asp 156 to the acetamide carbon of **3c** in Figure 2 indicates how a hydrogen bond could be envisioned by replacing the acetamide carbon atom with a NH group.

(17) Values were measured for all compounds against PKA, PKC, and c-Abl. All had IC_{50} values greater than 250 μM.

(18) Jeffrey, P. D.; Russo, A. A.; Polyak, K.; Gibbs, E.; Hurwitz, J.; Massague, J.; Pavletich, N. P. Mechanism of CDK activation revealed by the structure of a cyclin A CDK2 complex. *Nature* **1995**, *376*, 313−320.

(19) Sali, A.; Blundell, T. L. Comparative protein modeling by satisfaction of spatial restraints. *J. Mol. Biol.* **1993**, *234* (3), 779−815.

(20) Vriend, G. WHAT IF: a molecular modeling and drug design program. *J. Mol. Graphics* **1990**, *8* (1), 52−56.

(21) Schulze-Gahmen, U.; De Bondt, H. L.; Kim, S.-H. High-Resolution Crystal Structures of Human Cyclin-Dependent Kinase 2 with and without ATP: Bound Waters and Natural Ligand as Guides for Inhibitor Design. *J. Med. Chem.* **1996**, *39*, 4540−4546.

(22) Xu, X.; Nakano, T.; Wick, S.; Dubay, M.; Brizuela, L. Mechanism of CDK2/Cyclin E Inhibition by p27 and p27 Phosphorylation. *Biochemistry* **1999**, *38*, 8713−8722.

(23) Wick, S. T.; Dubay, M. M.; Imanil, I.; Brizuela, L. Biochemical and mutagenic analysis of the melanomatumor suppressor gene product/p16. *Oncogene* **1995**, *11*, 2013−2019.

(24) Carlson, B. A.; Dubay, M. M.; Sausville, E. A.; Brizuela, L.; Worland, P. J. Flavopiridol indices G1 arrest with inhibition of cyclin dependent kinase (CDK) 2 and CDK4 in human breast carcinoma cells. *Cancer Res.* **1996**, *56*, 2973−2978.

(25) Skehan, P.; Storeng, R.; Scudiero, D.; Monks, A.; McMahon, J.; Vistica, D.; Warren, J. T.; Bokesch, H.; Kenney, S.; Boyd, M. R. New colorimetric cytotoxicity assay for anticancer-drug screening. *J. Natl. Cancer Inst.* **1990**, *82* (13), 1107−1112.